

---

# Degree-Quant: Quantization-Aware Training for Graph Neural Networks

---

**Shyam A. Tailor\***  
Dept. of Computer Science  
University of Oxford

**Javier Fernandez-Marques\***  
Dept. of Computer Science  
University of Oxford

**Nicholas D. Lane**  
University of Cambridge  
Samsung AI Center

## Abstract

Graph neural networks (GNNs) have demonstrated strong performance on a wide variety of tasks due to their ability to model non-uniform structured data. Despite their promise, there exists little research exploring methods to make these architectures more efficient at inference time. In this work, we explore the viability of training quantized GNNs models, enabling the usage of low precision integer arithmetic during inference. We identify the sources of error that uniquely arise when attempting to quantize GNNs, and propose a method, *Degree-Quant*, to improve performance over existing quantization-aware training baselines commonly used on other architectures, such as CNNs. Models trained with Degree-Quant for INT8 quantization perform as well as FP32 models in most cases; for INT4 models, we obtain up to 69% gains over the baselines. Our work provides a comprehensive set of experiments across several datasets for node classification, graph classification and graph regression, laying strong foundations for future work in this area.

## 1 Introduction

Graph neural networks (GNNs) have received substantial attention in recent years due to their ability to model irregularly structured data. As a result, they are extensively used for applications as diverse as molecular interactions [10, 44], social networks [15], recommendation systems [38] or program understanding [3]. Recent advancements have centered around building more sophisticated models [30, 15, 40], including new types of layers [24, 39, 45] and better aggregation functions [8]. These have translated into better models overall, while keeping model sizes in the modest range of 0.1 MB, for 2-layer GCN network for Cora, to 0.32 MB, for FastGCN [7] on the much larger Reddit dataset. However, despite being small models in terms of number of parameters, the compute required for each application remains tightly coupled to the input graph size. A 2-layer GCN model with 32 hidden units would result in a model size of just 81KB but requires 19 GigaOPs to process the entire Reddit graph. We illustrate this growth in Figure 1.

One major challenge with graph architectures is therefore performing inference efficiently, which limits the applications they can be deployed for. For example, GNNs have been combined with CNNs for SLAM feature matching [35], however it is not possible to deploy this technique on smartphones, or even smaller devices, whose neural network accelerators often do not implement floating point arithmetic, and instead favour more efficient integer arithmetic. Integer quantization is one way to lower the compute budget required to perform inference, without necessarily requiring modifications to the model architecture. This is achieved by employing fewer bits to represent each element involved in the forward pass, significantly reducing memory consumption and data movement costs. Other benefits include faster inference and model compression.

Although quantization has been well studied for CNNs and language models [19, 42, 48, 32], there remains little work addressing GNN efficiency [31, 21]. To the best of our knowledge, there is no work studying quantization for GNNs, and explicitly characterising the issues that arise. The

---

\*Equal contribution

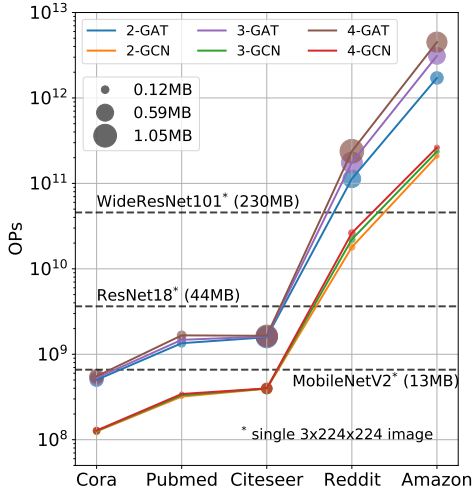


**Figure 1:** Despite GNN model sizes rarely exceeding 1MB, the OPs needed for inference grows at least linearly with the size of the dataset and node features. GNNs with models sizes  $100\times$  smaller than popular CNNs require many more OPs to process large graphs.

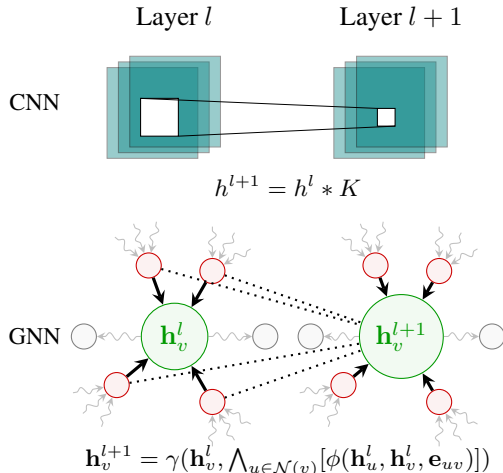


**Figure 2:** While CNNs operate on fixed, regular grids, GNNs operate on graphs with varying topology. A node’s neighborhood size and ordering varies for GNNs, unlike CNNs.

recent work of Wang et al. [41] explores only binarized embeddings of a single graph type (citation networks). Our work enables GNN quantization of any bit-width, which we evaluate under 8-bit and 4-bit settings and under six datasets including citation network node classification, superpixel image classification, molecular regression and social graph classification.

Architecturally, CNNs and GNNs have several similarities: most notably, they incorporate shared weights across nodes. However, while CNNs operate on a regular grid, and have a fixed neighbourhood, GNN nodes have neighborhoods that vary in size and do not have a fixed ordering. In a single graph, the variance in node degree can be substantial, which may cause the activations at GNN nodes to have a wider variance than would be observed at different spatial coordinates in a CNN architecture, where there is a fixed effective node degree. This lack of regularity makes the use of quantization less straightforward for GNNs.

This work provides the following contributions:

- The discovery and explanation of the sources of accuracy degradation in GNNs when using lower precision arithmetic. We analyse how the choice of straight-thought estimator (STE) implementation, node degree and method for tracking quantization statistics during training impacts performance.
- A method for quantization-aware training on graphs, *Degree-Quant* (DQ), which results in INT8 models often performing as well as their FP32 counterparts. At INT4, models typically outperform strong quantized baselines by over 20%. Our method enables a diverse range of architectures to be used without modifications to their aggregation functions.
- A comprehensive set of experiments studying the effects of quantization on GNNs, which has variable impact depending on layer architecture and dataset. We validate our findings on three popular architectures and six datasets for node classification, graph classification, regression applications and social networks.

## 2 Background

### 2.1 Message Passing Neural Networks (MPNNs)

Many popular GNN architectures may be viewed as generalizations of CNN architectures to an irregular domain: at a high level, graph architectures attempt to build representations based on a node’s neighborhood. Unlike CNNs, however, this neighborhood does not have a fixed ordering or

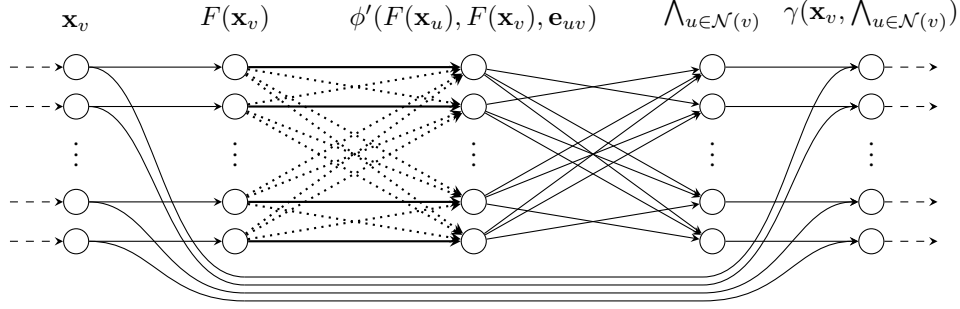


Figure 3: High level overview of stages in the message passing pipeline.

size. This work considers GNN architectures conforming to the MPNN paradigm [14]. A graph  $\mathcal{G}$  has node features  $\mathbf{X} \in \mathbb{R}^{N \times F}$ , an incidence matrix  $\mathbf{I} \in \mathbb{N}^{2 \times E}$ , and optionally  $D$ -dimensional edge features  $\mathbf{E} \in \mathbb{R}^{E \times D}$ . The forward pass through an MPNN layer consists of message passing, aggregation and update phases:  $\mathbf{x}'_v = \gamma(\mathbf{x}_v, \bigwedge_{u \in \mathcal{N}(v)} [\phi(\mathbf{x}_u, \mathbf{x}_v, \mathbf{e}_{uv})])$ . Messages from node  $u$  to node  $v$  are calculated using function  $\phi$ , and are aggregated using a permutation-invariant function  $\bigwedge$ . The features at  $v$  are subsequently updated using  $\gamma$ . This process is illustrated in Figure 3.

We focus on three architectures with corresponding update rules:

1. Graph Convolution Network (GCN):  $\mathbf{x}'_v = \sum_{u \in \mathcal{N}(v) \cup \{v\}} \left[ \frac{1}{\sqrt{\deg(u)\deg(v)}} \Theta \mathbf{x}_u \right]$  [24]
2. Graph Attention Network (GAT):  $\mathbf{x}'_v = \alpha_{v,v} \Theta \mathbf{x}_v + \sum_{u \in \mathcal{N}(v)} [\alpha_{v,u} \Theta \mathbf{x}_u]$ , where  $\alpha$  represent attention coefficients [39].
3. Graph Isomorphism Network (GIN):  $\mathbf{x}'_v = h_{\Theta}[(1 + \epsilon)\mathbf{x}_v + \sum_{u \in \mathcal{N}(v)} \mathbf{x}_u]$ , where  $h$  is a learnable function (e.g. a MLP) and  $\epsilon$  is a learnable constant [45].

## 2.2 Quantization for Non-Graph Neural Networks

Quantization allows for model size reduction and inference speedup without changing the model architecture. While there exists extensive studies of the impact of quantization at different bit-widths [9, 16, 28] and data formats [29, 6, 23], it is 8-bit integer (INT8) quantization that has attracted the most attention. This is due to INT8 models reaching comparable accuracy levels to full-precision (FP32) models [26, 19], offer a  $4\times$  model compression, and result in inference speedups on off-the-shelf hardware as 8-bit arithmetic is widely supported.

Quantization-aware training (QAT) has become the *de facto* approach towards designing robust quantized models with low error [42, 48, 42]. In their simplest forms, QAT schemes involve exposing the numerical errors introduced by quantization by simulating it on the forward pass and make use of a straight-through estimator (STE) [4] to compute the gradients—as if no quantization had been applied. For integer QAT, the quantization of a tensor  $x$  during the forward pass is often implemented as:  $x_q = \min(q_{\max}, \max(q_{\min}, \lfloor x/s + z \rfloor))$ , where  $q_{\min}$  and  $q_{\max}$  are the minimum and maximum representable values at a given bit-width and signedness,  $s$  is the scaling factor making  $x$  span the  $[q_{\min}, q_{\max}]$  range and,  $z$  is the *zero-point*, which allows for the real value 0 to be representable in  $x_q$ . Both  $s$  and  $z$  are scalars obtained at training time. Then, the tensor is *dequantized* as:  $\hat{x} = (x_q - z)s$ , where the resulting tensor  $\hat{x} \sim x$  for a high enough bit-width. This similarity degrades at lower bit-widths. Other variants of integer QAT are presented in Jacob et al. [19].

Reaching performance comparable to FP32 models at lower bit-widths is not trivial. As a result, QAT schemes often rely on other techniques such as *gradient clipping*, to mask gradient updates based on the largest representable value at a given bit-width; noisy QAT, which stochastically applies QAT to a portion of the weights at each training step [12]; or the re-ordering of layers [36, 2].

## 3 Quantization for GNNs

In this section, we build an intuition for why GNNs would fail with low precision arithmetic by identifying the sources of error that will disproportionately affect the accuracy of a low precision

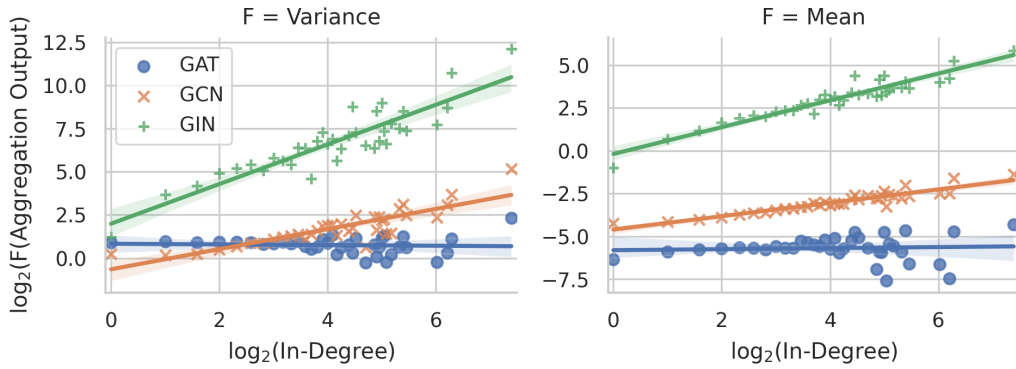


**Figure 4:** Analysis of values collected immediately after aggregation at the final layer of FP32 GNNs trained on Cora. Generated using channel data collected from 100 runs for each architecture. As in-degree grows, so does the mean and variance of channel values after aggregation.

model. Using this insight, we propose our novel technique for QAT with GNNs, *Degree-Quant*. In our analysis we focus on three models: GCN, GAT and GIN. This choice was made as we believe that these architectures are among the most popular graph architectures, with strong performance on a variety of tasks [11], while also being representative of different trends in graph architectures.

### 3.1 Sources of Error

QAT relies upon the STE to make an estimate of the gradient despite the non-differentiable rounding operation in the forward pass. If this approximation is inaccurate, however, then poor performance will be obtained. In GNN layers, we identify the aggregation phase, where nodes combine messages from a varying number of neighbors in a permutation-invariant fashion, as a source of substantial numerical error, especially at nodes with high in-degree due to two sources:

1. Outputs from aggregation have magnitudes that vary significantly depending on a node’s in-degree: as it increases, the variance of output values will increase. Over the course of training  $q_{\min}$  and  $q_{\max}$  may become severely distorted by infrequent outliers, reducing the resolution for the vast majority of values observed.
2. Accumulation at large in-degree nodes where errors compound will lead to the error being backpropagated to a large number of nodes, exacerbating the gradient error.

We can derive how the mean and variance of aggregation output values vary as node in-degree,  $n$ , increases for each of the three GNN layers, explaining the source (1) errors. Suppose we model incoming message values for a single output dimension with identically distributed random variables  $X_i$ , while making no assumptions on their exact distribution or independence. Further, we use  $Y_n$  as the random variable representing the value of node output after the aggregation step. With GIN layers, we have  $Y_n = (1 + \epsilon)X_0 + \sum_{i=1}^n X_i$ . It can be proven that  $\mathbb{E}(Y_n) = \mathcal{O}(n)$ . The variance is also proportion to  $n$  in the case that we assume that  $\sum_{i \neq j} \text{Cov}(X_i, X_j) \ll \sum_i \text{Var}(X_i)$ . This assumption is sensible: if  $\sum_{i \neq j} \text{Cov}(X_i, X_j)$  is large then it implies that the network has learned highly redundant features, and may be a sign of over-fitting. Similar arguments can be made for GCN and GAT layers; we would expect GCN aggregation values to grow with  $\mathcal{O}(\sqrt{n})$ , and GAT aggregation values to remain constant due to the attention coefficients.

We empirically validate these predictions on networks trained on the Cora dataset; results are plotted in fig. 4. We see from the log-log plot that the aggregation values do follow the trends predicted, and that for the values of in-degree in the plot (up to 168) the covariance terms can be neglected. As expected, the variance and mean of the aggregated output grow fastest for GIN, and are roughly constant for GAT as in-degree increases. From this empirical evidence, it would be expected that GIN layers are most affected by quantization, followed by GCN layers. GAT layers should be least affected, although they are still susceptible to source (2) errors.

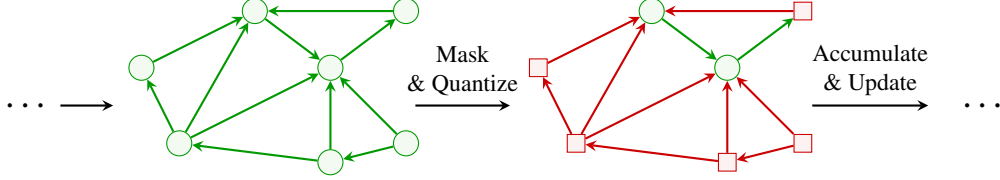


**Figure 5:** High-level view of the stochastic element of Degree-Quant. Masked (high in-degree) nodes, in green, operate at full precision, while unmasked nodes (red) operate at reduced precision. High in-degree nodes contribute most to poor gradient estimates, hence they are stochastically masked more often.

### 3.2 Our Method: Degree-Quant

To address these sources of error we propose *Degree-Quant* (DQ), a method for QAT with GNNs. Motivated by our observation that quantization error accumulates most at high in-degree nodes, our method targets these nodes specifically so that training can proceed successfully.

---

**Algorithm 1** Degree-Quant (DQ). Any function accepting the mask parameter  $\mathbf{m}$  is understood to perform only the masked computations at full precision: intermediate tensors are *not* quantized. At test time, all operations are performed at low precision.

---

```

1: procedure TRAINFORWARDPASS( $\mathcal{G}, \mathbf{p}$ )
2:    $\triangleright$  Calculate mask and quantized weights,  $\Theta'$ , which all operations share
3:    $\mathbf{m} \leftarrow \text{BERNOULLI}(\mathbf{p})$ 
4:    $\Theta' \leftarrow \text{QUANTIZE}(\Theta)$ 
5:    $\triangleright$  Messages with masked sources are at full precision (excluding weights)
6:    $\mathcal{M} \leftarrow \text{MESSAGECALCULATE}(\mathcal{G}, \Theta', \mathbf{m})$ 
7:    $X \leftarrow \text{QUANTIZE}(\text{AGGREGATE}(\mathcal{M}, \Theta', \mathbf{m}), \mathbf{m})$ 
8:   return UPDATE( $X, \Theta'$ ,  $\mathbf{m}$ )  $\triangleright$  Quantized weights always used
9: end procedure

```

---

DQ aims to encourage more accurate gradients to flow through high in-degree nodes by probabilistically performing the forward pass at those nodes at full precision. At each layer a binary node mask is generated; all masked nodes have the phases of the message passing, aggregation and update performed at full precision. This includes messages sent by masked nodes to other nodes, as shown in Figure 5. It is also important to note that the weights used at all nodes are the same quantized weights; this is motivated by the fact that our method is used to encourage more accurate gradients to flow back to the weights through high in-degree nodes. At test time masking is disabled: all nodes operate at low precision.

To generate the mask, we pre-process each graph before training and create a vector of probabilities  $\mathbf{p}$  with length equal to the number of nodes. At training time, mask  $\mathbf{m}$  is generated by sampling using the Bernoulli distribution:  $\mathbf{m} \sim \text{Bernoulli}(\mathbf{p})$ . In our scheme, the  $p_i$  is higher if the in-degree of node  $i$  is large. We use a simple scheme with two hyperparameters,  $p_{\min}$  and  $p_{\max}$ , to tune; nodes with the maximum in-degree are assigned  $p_{\max}$  as their masking probability, with all other nodes assigned a probability calculated by linearly interpolating between  $p_{\min}$  and  $p_{\max}$  based on their in-degree ranking in the graph.

Figure 4 also demonstrates large fluctuations in variance as in-degree increases. Since these fluctuations can disproportionately affect the ranges found by using min-max or momentum-based quantization, we propose using *percentiles*. While percentiles have been used for post-training quantization (PTQ) [43], we are the first (to the best of our knowledge) to propose making it a core part of QAT; we find it to be a key contributor to achieving good results with graphs. We are more aggressive than existing literature on the quantity we discard: we clip the top and bottom 0.1%, rather than 0.01%, as we observe the fluctuations to be a larger issue with GNNs than with CNNs or DNNs. Quantization ranges are more representative of the vast majority of values in this scheme, resulting in greater precision as bits are not wasted for encoding infrequently observed values.

We note that a core contribution of DQ is to enable a diverse range of aggregation functions to be usable at lower precision: recent work demonstrates that the choice of aggregation function impacts the model’s representational capacity [45], and they have significantly different computational

Dataset	Model Arch.	STE		Gradient Clipping	
		min/max	momentum	min/max	momentum
Cora (Acc. %) $\uparrow$	GCN	<b>81.03 <math>\pm</math> 0.7</b>	42.32 $\pm$ 11.1	80.84 $\pm$ 0.8	66.94 $\pm$ 18.2
	GAT	76.04 $\pm$ 2.2	81.73 $\pm$ 1.3	76.44 $\pm$ 2.6	<b>81.91 <math>\pm</math> 0.7</b>
	GIN	69.86 $\pm$ 1.9	49.15 $\pm$ 10.2	69.17 $\pm$ 2.3	<b>75.14 <math>\pm</math> 1.1</b>
MNIST (Acc. %) $\uparrow$	GCN	<b>90.44 <math>\pm</math> 0.2</b>	90.06 $\pm$ 0.5	90.44 $\pm$ 0.3	90.21 $\pm$ 0.4
	GAT	<b>95.77 <math>\pm</math> 0.1</b>	95.73 $\pm$ 0.3	95.72 $\pm$ 0.1	95.65 $\pm$ 0.3
	GIN	96.45 $\pm$ 0.3	<b>96.72 <math>\pm</math> 0.2</b>	96.36 $\pm$ 0.4	75.32 $\pm$ 18.1
ZINC (Loss) $\downarrow$	GCN	0.4855 $\pm$ 0.01	0.5093 $\pm$ 0.01	0.4945 $\pm$ 0.01	<b>0.4825 <math>\pm</math> 0.01</b>
	GAT	0.4711 $\pm$ 0.01	0.5714 $\pm$ 0.03	0.4658 $\pm$ 0.01	<b>0.4626 <math>\pm</math> 0.01</b>
	GIN	0.3926 $\pm$ 0.02	<b>0.3858 <math>\pm</math> 0.03</b>	0.3901 $\pm$ 0.02	0.3882 $\pm$ 0.02

**Table 1:** Impact on performance of four STE variants when using INT8 quantization. Momentum is set to default 0.01. In bold the STE configuration that resulted in best performing models for each dataset-model pair. Hyperparameters for each experiment were fine-tuned independently.

requirements. Although GAT layers are not as susceptible as other types of layers to degradation, they are slow due to the expensive attention coefficient calculation [11].

## 4 Experiments

In this section we first analyse on how the choice of STE affects performance for GNNs. We subsequently evaluate Degree-Quant against strong FP32 and INT8-QAT baselines. Our study evaluates performance on six datasets and includes both node-level and graph-level tasks. The datasets used were Cora, CiteSeer [47], ZINC [22], MNIST and CIFAR10 superpixels [25], and REDDIT-BINARY [46].

Across all datasets INT8 models trained with Degree-Quant manage to recover most of the accuracy lost as a result of quantization. In some instances, DQ-INT8 outperform the FP32 baselines. For INT4, DQ results in double digits improvements over QAT-INT4. Details about each dataset and our experimental setup can be found in appendix A.1. We report the mean and standard deviation for each experiment.

### 4.1 Impact of Gradient Estimator on Convergence

The STE is a workaround for when the forward pass contains non-differentiable operations (e.g. rounding in QAT) that has been widely adopted in practice. While the choice of STE implementation generally results in marginal differences for CNNs—even for binary networks [2]—it is unclear whether only marginal differences will also be observed for GNNs. Motivated by this, we study the impact of four STE variants on the three architectures evaluated for each type of dataset; the implementation of each STE configuration is described in appendix A.3. We perform this experiment to ensure that we have the strongest possible QAT baselines. Results are shown in table 1. We found the choice of STE configuration to be highly dependent on the model architecture and type of problem to be solved: we see a much larger variance than is observed with CNNs; this is an important discovery for future work building on our study.

For Cora, large gradient norm values in the early stages of training (see fig. 6) mean that these models not benefit from momentum as quantization ranges fail to keep up with the rate of changes in tensor values; higher momentum can help but also leads to instability. In contrast, GAT has stable initial training dynamics, and hence obtains better results with momentum, as it is less susceptible to the variance issue previously discussed. We see that gradient clipping can be beneficial if using momentum, as it dampens initial training dynamics.

For the remaining datasets there is no strong trend favouring STE or gradient clipping, indicating it is not an important factor when training models to generalize to new graphs. However, we see a general trend favouring momentum on ZINC, which we do not see on MNIST. As ZINC has a more tailed in-degree distribution than MNIST (fig. 10), we expect outliers to arise more commonly when training on ZINC. As momentum is more robust to these outliers it provides a clear benefit on ZINC.

Quant. Scheme	Model Arch.	Node Classification (Accuracy %)		Graph Classification (Accuracy %)		Graph Regression (Loss)
		Cora $\uparrow$	Citeseer $\uparrow$	MNIST $\uparrow$	CIFAR-10 $\uparrow$	ZINC $\downarrow$
Ref. (FP32)	GCN	81.4 $\pm$ 0.7	71.1 $\pm$ 0.7	90.0 $\pm$ 0.2	54.5 $\pm$ 0.1	0.469 $\pm$ 0.002
	GAT	83.1 $\pm$ 0.4	70.8 $\pm$ 0.5	95.6 $\pm$ 0.1	65.4 $\pm$ 0.4	0.463 $\pm$ 0.002
	GIN	77.6 $\pm$ 1.1	66.1 $\pm$ 0.9	93.9 $\pm$ 0.6	53.3 $\pm$ 3.7	0.414 $\pm$ 0.009
Ours (FP32)	GCN	80.9 $\pm$ 0.7	71.4 $\pm$ 0.9	90.9 $\pm$ 0.4	58.4 $\pm$ 0.5	0.450 $\pm$ 0.008
	GAT	82.3 $\pm$ 0.8	70.5 $\pm$ 0.9	95.8 $\pm$ 0.4	65.1 $\pm$ 0.8	0.455 $\pm$ 0.006
	GIN	77.9 $\pm$ 1.1	65.1 $\pm$ 2.1	96.4 $\pm$ 0.4	57.4 $\pm$ 0.7	0.334 $\pm$ 0.024
QAT (INT8)	GCN	81.0 $\pm$ 0.7	70.9 $\pm$ 0.7	90.9 $\pm$ 0.2	56.4 $\pm$ 0.5	0.481 $\pm$ 0.029
	GAT	81.9 $\pm$ 0.7	70.5 $\pm$ 0.9	95.8 $\pm$ 0.3	66.3 $\pm$ 0.4	0.460 $\pm$ 0.005
	GIN	75.6 $\pm$ 1.2	63.0 $\pm$ 2.6	96.7 $\pm$ 0.2	52.4 $\pm$ 1.2	0.386 $\pm$ 0.025
DQ (INT8)	GCN	81.7 $\pm$ 0.7 (+0.7)	70.7 $\pm$ 0.9 (-0.2)	90.9 $\pm$ 0.1 (+0.0)	56.3 $\pm$ 0.1 (-0.1)	0.434 $\pm$ 0.009 (+9.8)
	GAT	82.1 $\pm$ 0.1 (+0.2)	70.8 $\pm$ 1.0 (+0.3)	95.8 $\pm$ 0.4 (+0.0)	67.7 $\pm$ 0.5 (+1.4)	0.456 $\pm$ 0.005 (+0.9)
	GIN	77.2 $\pm$ 1.2 (+1.6)	67.4 $\pm$ 1.4 (+4.4)	96.6 $\pm$ 0.4 (-0.1)	55.5 $\pm$ 0.6 (+3.1)	0.357 $\pm$ 0.014 (+7.5)

**Table 2:** Results for DQ at INT8, with percent points improvements over baseline QAT in bold (for ZINC we show relative improvement). We obtain FP32 baselines better than previously reported in many cases due to extensive hyperparameter tuning. While GCN and GAT models retain most accuracy for INT8, models with GIN layers result in larger degradations. Models trained with Degree-Quant (DQ), result in performances comparable to those of their FP32 counterparts, with better performance than FP32 baselines in some cases.

## 4.2 Experimental Results for Degree-Quant

Our FP32 baselines achieved better performance after tuning the hyperparameters used in the reference FP32 implementations. We observed significant gains for GIN models for MNIST (2.5%) and CIFAR10 (4.1%) and large gains for all models on the ZINC dataset (mean 10%). In the case of citation networks, our hyperparameter tuning resulted in models with considerably lower validation loss, however that did not translate into higher test accuracy. Our FP32 results and those from the baselines are shown at the top of table 2. Our results with DQ are highlighted in gray.

For our QAT-INT8 baselines, we use STE configurations informed by our analysis in section 4.1. For Citeseer we use the best resulting setup analysed for Cora, and for CIFAR-10 that from MNIST. Then, the hyperparameters for each experiment were fine tuned individually. QAT-INT8 results in table 2, with the exception of MNIST (an easy to classify dataset), corroborate our hypothesis that GIN layers are less resilient to quantization. This was first observed in fig. 4. In the case of ZINC, while all models results in noticeable degradation, GIN sees a more severe 16% increase of regression loss compared to our FP32 baseline.

Citation networks trained with DQ manage to recover most of the accuracy lost as a results of QAT-INT8. In some instances DQ-INT8 models outperform the reference FP32 baselines. We see DQ being more effective for GIN layers, outperforming INT8 baselines for Citeseer (4.4%) and REDDIT-BINARY (15.7%) by large margins. Among the top performing models using DQ, ratios of  $p_{\min}$  and  $p_{\max}$  in  $[0.0, 0.2]$  were the most common. Figure 11 in the appendix shows validation loss curves for GIN models trained using different DQ probabilities on the REDDIT-BINARY dataset.

Quant.	Model	Citeseer (Acc. %) $\uparrow$	ZINC (Loss) $\downarrow$
QAT (INT4)	GCN	65.7 $\pm$ 3.2	0.678 $\pm$ 0.014
	GAT	65.3 $\pm$ 1.9	0.655 $\pm$ 0.032
	GIN	18.6 $\pm$ 2.9	1.390 $\pm$ 0.164
DQ (INT4)	GCN	66.9 $\pm$ 2.4 (+1.2)	0.533 $\pm$ 0.010 (+21.4)
	GAT	67.6 $\pm$ 1.5 (+2.3)	0.520 $\pm$ 0.021 (+20.6)
	GIN	60.8 $\pm$ 2.1 (+42.2)	0.431 $\pm$ 0.012 (+69.0)

**Table 3:** DQ for INT4 significantly reduced the loss for ZINC (shown relative improvement), outperforming some of the FP32 baselines. For Citeseer, results outperform the INT4 baselines by large margins, specially for GIN.

Quantization	Model	REDDIT-BIN (Acc. %) $\uparrow$
Ref. (FP32)	GIN	92.2 $\pm$ 2.3
Ours (FP32)	GIN	92.0 $\pm$ 1.5
QAT-INT8	GIN	76.1 $\pm$ 7.5
DQ-INT8	GIN	91.8 $\pm$ 2.3 (+15.7)
QAT-INT4	GIN	54.4 $\pm$ 6.6
DQ-INT4	GIN	81.3 $\pm$ 4.4 (+26.9)

**Table 4:** Results for DQ-INT8 GIN models perform nearly as well as at FP32. For INT4, DQ offers a significant increase in accuracy. We focus on GIN as it is most susceptible to degradation.

## 5 Discussion

### Performance Implications

The performance benefits of INT8 arithmetic have been well studied for CNNs and other *regular* architectures [17]. It is reasonable to expect a  $1.5\times$  to  $2\times$  CPU acceleration [19, 5] and up to  $10\times$  GPU acceleration [20]. However, we note that to obtain peak performance it is necessary to process nodes with a cache-friendly ordering: the true speedup will be dataset and hardware dependent. While it is trivial to derive a processing order for regular graphs (e.g. images), it is more difficult for irregular topologies. Existing literature has explored efficient graph processing techniques [34], however they have not been applied to GNNs. We leave finding an efficient processing ordering as future work. It is also worth emphasizing that quantized networks are necessary to use accelerators deployed in smartphones and smaller devices as they primarily accelerate integer arithmetic. Quantized networks are also smaller and require less memory at inference-time, by a factor of  $4\times$  with INT8; this is especially relevant for GNNs operating on large graphs, as memory is at a premium in accelerators.

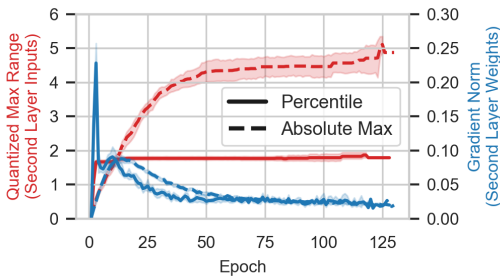


**Figure 6:**  $q_{\max}$  with absolute min/max and percentile ranges, applied to INT8 GCN training on Cora. We observe that the percentile max is half that of the absolute, doubling resolution for the majority of values.

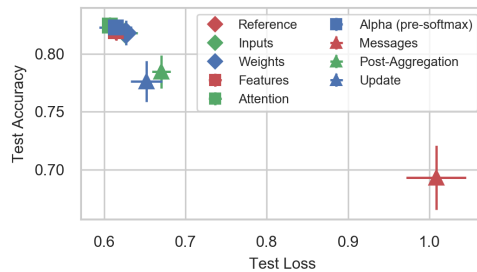


**Figure 7:** Analysis of how INT8 GAT performance degrades on Cora as individual elements are reduced to 4-bit precision. For GAT the message elements are most crucial to classification performance.

### Benefits of Percentile Ranges

Figure 6 demonstrates the importance of using percentiles during training. We see that when using standard absolute min/max that the upper range grows to over double the range required for 99.9% of values: this effectively halves the quantization resolution for most values. We found that gradient clipping had no clear benefits when combined with percentiles: all results used the STE, with the exception of REDDIT-BINARY. DQ was also far more stable, and we obtained strong results with an order of magnitude less tuning relative to the QAT baselines.

### Ablation Study: Moving to INT4

Figure 7 assesses how INT8 GAT degrades as single elements are converted to INT4. This allows us to study which elements are most affected by further quantization; further plots for GCN and GIN are included in the appendix. We observe that most elements cause only modest performance losses relative to a full INT8 model. However, we see that quantizing messages (i.e.  $\alpha_{v,u} \Theta x_u$ ) causes significant degradation, but quantizing neither the feature weights or attention weights caused significant accuracy loss. A similar trend can be seen for GCN and GIN: significant model compression is achievable. *Numerical precision* is the limiting factor for existing architectures. In general we find it useful to increase the percentile from 0.1% to 1% at INT4 for bottleneck elements shown in the ablation plots. We provide results for full INT4 models in tables 3 and 4, with consistent gains of over 20%.

### Ablation Study: Effect of Stochastic Element in Degree-Quant

We observe that the stochastic masking in DQ alone often achieves most of the performance gain over the QAT baseline; results are given in table 9 in the appendix. The benefit of the percentile-based quantization ranges is primarily for stability, although it can yield some performance gains. The full DQ method provides consistently good results on all architectures and datasets, without requiring an extensive search used in section 4.1.

## 6 Conclusion

This work has presented Degree-Quant, a method for training a diverse set of GNN architectures to obtain close to FP32 performance while using only 8-bit integer arithmetic. Our work is a first step towards enabling GNNs to be deployed more widely, including to resource constrained devices such as smartphones. We believe that our insights pave the way for research into mixed-precision training and further techniques for efficient inference with GNNs.

### Broader Impact

Our work focuses on how to train graph neural network (GNN) architectures so that inference can be performed with low precision arithmetic. The primary benefits of this are model compression, reduced memory consumption, and inference acceleration. These may allow graph architectures to run on more resource-constrained devices, such as smartphones, in the future. Enabling machine learning models to be used on these devices can enable a simple, yet strong, privacy model as data does not have to be offloaded to the cloud for inference. However, ubiquity may enable mass surveillance, but we note that this drawback is not exclusive to graph architectures but to all research seeking for efficient deployments of machine learning systems. Our work may also enable more sophisticated GNNs to be run on datacenter class hardware for production use-cases. There are both positive (drug discovery) and negative (surveillance) applications for more sophisticated models, but this is true of any work exploring efficiency for deep learning systems.

Our technique, Degree-Quant (DQ), is motivated by observations about graph topology. Naive quantization disproportionately affects high in-degree nodes; however, the stochastic element of our method specifically targets them to improve performance. As mentioned in the discussion, it is observed that this stochastic element is responsible for most of the performance gain over the quantized baseline. Overall, our method improves performance at these high in-degree nodes, which leads to substantial improvements for both node-level and graph-level tasks. We note, however, that quantization for GNNs may disproportionately affect individual nodes, and practitioners should be careful to ensure that this degradation does not disadvantage any individuals for their specific application—for example, if the graph is a social graph. This downside is *alleviated* by DQ, but may still be present.

### Acknowledgments and Disclosure of Funding

This work was supported by Samsung AI, Arm and, by the UK’s Engineering and Physical Sciences Research Council (EPSRC) with grants EP/M50659X/1 and EP/S001530/1.

### References

- [1] R. Achanta, A. Shaji, K. Smith, A. Lucchi, P. Fua, and S. Süsstrunk. Slic superpixels compared to state-of-the-art superpixel methods. *IEEE Transactions on Pattern Analysis and Machine Intelligence*, 34(11):2274–2282, 2012.
- [2] Milad Alizadeh, Javier Fernández-Marqués, Nicholas D. Lane, and Yarin Gal. A empirical study of binary neural networks’ optimisation. In *International Conference on Learning Representations*, 2019. URL <https://openreview.net/forum?id=rJfUCoR5KX>.
- [3] Miltiadis Allamanis, Marc Brockschmidt, and Mahmoud Khademi. Learning to represent programs with graphs. In *6th International Conference on Learning Representations, ICLR 2018, Vancouver, BC, Canada, April 30 - May 3, 2018, Conference Track Proceedings*. OpenReview.net, 2018. URL <https://openreview.net/forum?id=BJ0FETxR->.
- [4] Yoshua Bengio, Nicholas Léonard, and Aaron Courville. Estimating or propagating gradients through stochastic neurons for conditional computation, 2013.
- [5] Aishwarya Bhandare, Vamsi Sripathi, Deepthi Karkada, Vivek Menon, Sun Choi, Kushal Datta, and Vikram Salelore. Efficient 8-bit quantization of transformer neural machine language translation model, 2019.
- [6] Zachariah Carmichael, Hamed F. Langroudi, Char Khazanov, Jeffrey Lillie, John L. Gustafson, and Dhireesha Kudithipudi. Deep positron: A deep neural network using the posit number system, 2018.

- [7] Jie Chen, Tengfei Ma, and Cao Xiao. Fastgcn: Fast learning with graph convolutional networks via importance sampling, 2018.
- [8] Gabriele Corso, Luca Cavalleri, Dominique Beaini, Pietro Liò, and Petar Veličković. Principal neighbourhood aggregation for graph nets, 2020.
- [9] Matthieu Courbariaux, Yoshua Bengio, and Jean-Pierre David. Binaryconnect: Training deep neural networks with binary weights during propagations, 2015.
- [10] David K Duvenaud, Dougal Maclaurin, Jorge Iparraguirre, Rafael Bombarell, Timothy Hirzel, Alán Aspuru-Guzik, and Ryan P Adams. Convolutional networks on graphs for learning molecular fingerprints. In *Advances in neural information processing systems*, pp. 2224–2232, 2015.
- [11] Vijay Prakash Dwivedi, Chaitanya K. Joshi, Thomas Laurent, Yoshua Bengio, and Xavier Bresson. Benchmarking graph neural networks, 2020.
- [12] Angela Fan, Pierre Stock, Benjamin Graham, Edouard Grave, Remi Gribonval, Herve Jegou, and Armand Joulin. Training with quantization noise for extreme model compression, 2020.
- [13] Matthias Fey and Jan Eric Lenssen. Fast graph representation learning with pytorch geometric, 2019.
- [14] Justin Gilmer, Samuel S. Schoenholz, Patrick F. Riley, Oriol Vinyals, and George E. Dahl. Neural message passing for quantum chemistry. *CoRR*, abs/1704.01212, 2017. URL <http://arxiv.org/abs/1704.01212>.
- [15] William L. Hamilton, Rex Ying, and Jure Leskovec. Inductive representation learning on large graphs, 2017.
- [16] Song Han, Huizi Mao, and William J. Dally. Deep compression: Compressing deep neural networks with pruning, trained quantization and huffman coding, 2015.
- [17] M. Horowitz. 1.1 computing’s energy problem (and what we can do about it). In *2014 IEEE International Solid-State Circuits Conference Digest of Technical Papers (ISSCC)*, pp. 10–14, Feb 2014. doi: 10.1109/ISSCC.2014.6757323.
- [18] Sergey Ioffe and Christian Szegedy. Batch normalization: Accelerating deep network training by reducing internal covariate shift, 2015.
- [19] Benoit Jacob, Skirmantas Kligys, Bo Chen, Menglong Zhu, Matthew Tang, Andrew Howard, Hartwig Adam, and Dmitry Kalenichenko. Quantization and training of neural networks for efficient integer-arithmetic-only inference, 2017.
- [20] Zhe Jia, Marco Maggioni, Jeffrey Smith, and Daniele Paolo Scarpazza. Dissecting the nvidia turing t4 gpu via microbenchmarking, 2019.
- [21] Zhihao Jia, Sina Lin, Mingyu Gao, Matei Zaharia, and Alex Aiken. Improving the accuracy, scalability, and performance of graph neural networks with roc. In *Proceedings of Machine Learning and Systems 2020*, pp. 187–198. 2020.
- [22] Wengong Jin, Regina Barzilay, and Tommi Jaakkola. Junction tree variational autoencoder for molecular graph generation, 2018.
- [23] Dhiraj Kalamkar, Dheevatsa Mudigere, Naveen Mellempudi, Dipankar Das, Kunal Banerjee, Sasikanth Avancha, Dharma Teja Vooturi, Nataraj Jammalamadaka, Jianyu Huang, Hector Yuen, Jiyan Yang, Jongsoo Park, Alexander Heinecke, Evangelos Georganas, Sudarshan Srinivasan, Abhisek Kundu, Misha Smelyanskiy, Bharat Kaul, and Pradeep Dubey. A study of bfloat16 for deep learning training, 2019.
- [24] Thomas N. Kipf and Max Welling. Semi-supervised classification with graph convolutional networks. In *5th International Conference on Learning Representations, ICLR 2017, Toulon, France, April 24-26, 2017, Conference Track Proceedings*. OpenReview.net, 2017. URL <https://openreview.net/forum?id=SJU4ayYg1>.
- [25] Boris Knyazev, Graham W. Taylor, and Mohamed R. Amer. Understanding attention and generalization in graph neural networks, 2019.
- [26] Raghuraman Krishnamoorthi. Quantizing deep convolutional networks for efficient inference: A whitepaper, 2018.
- [27] Liam Li, Kevin Jamieson, Afshin Rostamizadeh, Ekaterina Gonina, Jonathan Ben-tzur, Moritz Hardt, Benjamin Recht, and Ameet Talwalkar. A system for massively parallel hyperparameter tuning. In *Proceedings of Machine Learning and Systems 2020*, pp. 230–246. 2020.
- [28] Christos Louizos, Karen Ullrich, and Max Welling. Bayesian compression for deep learning, 2017.
- [29] Paulius Micikevicius, Sharan Narang, Jonah Alben, Gregory Diamos, Erich Elsen, David Garcia, Boris Ginsburg, Michael Houston, Oleksii Kuchaiev, Ganesh Venkatesh, and Hao Wu. Mixed precision training, 2017.

- [30] Federico Monti, Davide Boscaini, Jonathan Masci, Emanuele Rodolà, Jan Svoboda, and Michael M. Bronstein. Geometric deep learning on graphs and manifolds using mixture model cnns, 2016.
- [31] Anurag Mukkara, Nathan Beckmann, Maleen Abeydeera, Xiaosong Ma, and Daniel Sanchez. Exploiting locality in graph analytics through hardware-accelerated traversal scheduling. In *Proceedings of the 51st Annual IEEE/ACM International Symposium on Microarchitecture*, MICRO-51, pp. 1–14. IEEE Press, 2018. ISBN 9781538662403. doi: 10.1109/MICRO.2018.00010. URL <https://doi.org/10.1109/MICRO.2018.00010>.
- [32] Gabriele Prato, Ella Charlaix, and Mehdi Rezagholizadeh. Fully quantized transformer for machine translation, 2019.
- [33] Yu Rong, Wenbing Huang, Tingyang Xu, and Junzhou Huang. Dropedge: Towards deep graph convolutional networks on node classification. In *International Conference on Learning Representations*, 2020. URL <https://openreview.net/forum?id=Hkx1qkrKPr>.
- [34] Amitabha Roy, Ivo Mihailovic, and Willy Zwaenepoel. X-stream: Edge-centric graph processing using streaming partitions. In *Proceedings of the Twenty-Fourth ACM Symposium on Operating Systems Principles*, pp. 472–488, 2013.
- [35] Paul-Edouard Sarlin, Daniel DeTone, Tomasz Malisiewicz, and Andrew Rabinovich. Superglue: Learning feature matching with graph neural networks. *arXiv preprint arXiv:1911.11763*, 2019.
- [36] Tao Sheng, Chen Feng, Shaojie Zhuo, Xiaopeng Zhang, Liang Shen, and Mickey Aleksic. A quantization-friendly separable convolution for mobilenets. *2018 1st Workshop on Energy Efficient Machine Learning and Cognitive Computing for Embedded Applications (EMC2)*, Mar 2018. doi: 10.1109/emc2.2018.00011. URL <http://dx.doi.org/10.1109/emc2.2018.00011>.
- [37] Nitish Srivastava, Geoffrey Hinton, Alex Krizhevsky, Ilya Sutskever, and Ruslan Salakhutdinov. Dropout: a simple way to prevent neural networks from overfitting. *The journal of machine learning research*, 15(1): 1929–1958, 2014.
- [38] Rianne van den Berg, Thomas N. Kipf, and Max Welling. Graph convolutional matrix completion, 2017.
- [39] Petar Velickovic, Guillem Cucurull, Arantxa Casanova, Adriana Romero, Pietro Liò, and Yoshua Bengio. Graph attention networks. In *6th International Conference on Learning Representations, ICLR 2018, Vancouver, BC, Canada, April 30 - May 3, 2018, Conference Track Proceedings*. OpenReview.net, 2018. URL <https://openreview.net/forum?id=rJXmpikCZ>.
- [40] Petar Veličković, William Fedus, William L. Hamilton, Pietro Liò, Yoshua Bengio, and R Devon Hjelm. Deep graph infomax, 2018.
- [41] Hanchen Wang, Defu Lian, Ying Zhang, Lu Qin, Xiangjian He, Yiguang Lin, and Xuemin Lin. Binarized graph neural network, 2020.
- [42] Kuan Wang, Zhijian Liu, Yujun Lin, Ji Lin, and Song Han. Haq: Hardware-aware automated quantization with mixed precision, 2018.
- [43] Hao Wu, Patrick Judd, Xiaojie Zhang, Mikhail Isaev, and Paulius Micikevicius. Integer quantization for deep learning inference: Principles and empirical evaluation, 2020.
- [44] Zhenqin Wu, Bharath Ramsundar, Evan N. Feinberg, Joseph Gomes, Caleb Geniesse, Aneesh S. Pappu, Karl Leswing, and Vijay Pande. Moleculenet: A benchmark for molecular machine learning, 2017.
- [45] Keyulu Xu, Weihua Hu, Jure Leskovec, and Stefanie Jegelka. How powerful are graph neural networks? In *7th International Conference on Learning Representations, ICLR 2019, New Orleans, LA, USA, May 6-9, 2019*. OpenReview.net, 2019. URL <https://openreview.net/forum?id=ryGs6iA5Km>.
- [46] Pinar Yanardag and S.V.N. Vishwanathan. Deep graph kernels. In *Proceedings of the 21th ACM SIGKDD International Conference on Knowledge Discovery and Data Mining, KDD '15*, pp. 1365–1374, New York, NY, USA, 2015. Association for Computing Machinery. ISBN 9781450336642. doi: 10.1145/2783258.2783417. URL <https://doi.org/10.1145/2783258.2783417>.
- [47] Zhilin Yang, William W. Cohen, and Ruslan Salakhutdinov. Revisiting semi-supervised learning with graph embeddings, 2016.
- [48] Ofir Zafrir, Guy Boudoukh, Peter Izsak, and Moshe Wasserblat. Q8bert: Quantized 8bit bert, 2019.

## A Appendix

### A.1 Experimental Setup

As baselines we use the architectures and results reported by Fey & Lenssen [13] for citation networks, Dwivedi et al. [11] for MNIST, CIFAR-10 and ZINC and, Xu et al. [45] for REDDIT-BINARY. We re-implemented the architectures and datasets used in these publications and replicated the results reported at FP32. Models using GIN layers learn parameter  $\epsilon$ . These models are often referred to as GIN- $\epsilon$ . The high-level description of these architectures is shown in table 5. The number of parameters for each architecture-dataset in this work are shown in table 6.

Our infrastructure was implemented using PyTorch Geometric (PyG) [13]. We generate candidate hyperparameters using random search, and prune trials using the asynchronous hyperband algorithm [27]. Hyperparameters searched over were learning rate, weight decay, and dropout [37] and drop-edge [33] probabilities. The search ranges were initialized centered at the values used in the reference implementations of the baselines. Degree-Quant requires searching for two additional hyperparameters,  $p_{\min}$  and  $p_{\max}$ , these were tuned in a grid-search fashion. We report our results using the hyperparameters which achieved the best validation loss over 100 runs on the Cora and Citeseer datasets, 10 runs for MNIST, CIFAR-10 and ZINC, and 10-fold cross-validation for REDDIT-BINARY.

Our experiments ran on several machines in our SLURM cluster using Intel CPUs and NVIDIA GPUs. Each machine was running Ubuntu 18.04. The GPU models in our cluster were: V100, RTX 2080Ti and GTX 1080Ti.

Model Arch.	# Layers					# Hidden Units					Residual					Output MLP				
	Cit	M	C	Z	R	Cit	M	C	Z	R	Cit	M	C	Z	R	Cit	M	C	Z	R
GCN	2	4	4	4	-	16	146	146	145	-	×	✓	✓	✓	-	×	✓	✓	✓	-
GAT	2	4	4	4	-	8	19	19	18	-	×	✓	✓	✓	-	×	✓	✓	✓	-
GIN	2	4	4	4	5	16	110	110	110	64	×	✓	✓	✓	×	×	✓	✓	✓	✓

**Table 5:** High level description of the architectures evaluated for citation networks (Cit), MNIST (M), CIFAR-10 (C), ZINC (Z) and REDDIT-BINARY (R). We relied on Adam optimizer for all experiments. For all batched experiments, we used 128 batch-sizes. All GAT models used 8 attention heads. All GIN architectures used 2-layer MLPs, except those for citation networks which used a single linear layer.

Model Arch.	Node Classification		Graph Classification			Graph Regression
	Cora	Citeseer	MNIST	CIFAR-10	REDDIT-BIN	ZINC
GCN	23063	59366	103889	104181	-	105454
GAT	92373	237586	113706	114010	-	105044
GIN	23216	59536	104554	104774	42503	102088

**Table 6:** Number of parameters for each of the evaluated architectures

For QAT experiments, all elements of each network are quantized: inputs to each layer, the weights, the messages sent between nodes, the inputs to aggregation stage and its outputs and, the outputs of the update stage (which are the outputs of the GNN layer before activation). In this way, all intermediate tensors in GNNs are quantized with the exception of the attention mechanism in GAT; we do not quantize after the softmax calculation, due to the numerical precision required at this stage. With the exception of Cora and Citeseer, the models evaluated in this work make use of Batch Normalization [18]. For deployments of quantized models, Batch Normalization layers are often *folded* with the weights [26]. This is to ensure the input to the next layer is within the expected  $[q_{\min}, q_{\max}]$  ranges. In this work, for both QAT baselines and QAT+DQ, we left BN layers unfolded but ensure the inputs and outputs were quantized to the appropriate number of bits (i.e. INT8 or INT4) before getting multiplied with the layer weights. We leave as future work proposing a BN folding mechanism applicable for GNNs and studying its impact for deployments of quantized GNNs.

The GIN models evaluated on REDDIT-BINARY used QAT for all layers with the exception of the input layer of the MLP in the first GIN layer. This compromise was needed to overcome the severe degradation introduced by quantization when operating on nodes with a single scalar as feature.

## A.2 Datasets

We show in Table 7 the statistics for each dataset either used or referred to in this work. For Cora and Citeseer datasets, nodes correspond to documents and edges to citations between these. Node features are a bag-of-words representation of the document. The task is to classify each node in the graph (i.e. each document) correctly. The MNIST and CIFAR-10 datasets (commonly used for image classification) are transformed using SLIC [1] into graphs where each node represents a cluster of perceptually similar pixels or superpixels. The task is to classify each image using their superpixels graph representation. The ZINC dataset contains graphs representing molecules, where each node is an atom. The task is to regress a molecular property (constrained solubility [22]) given the graph representation of the molecule. Nodes in graphs of the REDDIT-BINARY dataset represent users of a Reddit thread with edges drawn between a pair of nodes if these interacted. This dataset contains graphs of two types of communities: question-answer threads and discussion threads. The task is to determine if a given graph is from a question-answer thread or a discussion thread.

We use standard splits for MNIST, CIFAR-10 and ZINC. For citation datasets (Cora and Citeseer), we use the splits used by Kipf & Welling [24]. For REDDIT-BINARY we use 10-fold cross validation.

Dataset	Graphs	Nodes	Edges	Features	Labels
Cora	1	2,708	5,278	1,433	7
Citeseer	1	3,327	4,552	3,703	6
Pubmed	1	19,717	108,365	500	3
MNIST	70K	40-75	564.53 (avg)	3	10
CIFAR10	60K	85-150	941.07 (avg)	5	10
ZINC	12K	9-37	49.83 (avg)	28	1
REDDIT-BINARY	2K	429.63 (avg)	497.75 (avg)	1	2
Reddit	1	232,965	114,848,857	602	41
Amazon	1	9,430,088	231,594,310	300	24

**Table 7:** Statistics for each dataset used in the paper. Some datasets are only referred to in fig. 1

## A.3 STE Configurations

In section 4.1 we analyse different configurations of STE and how they impact in QAT results. First, vanilla STE, which is the reference STE implementation [4] that lets the gradients pass unchanged; and gradient clipping (GC), which clips the gradients based on the maximum representable value for a given quantization level. Or in other words, GC limits gradients if the tensor’s magnitudes are outside the  $[q_{\min}, q_{\max}]$  range.

$$x_{\min} = \begin{cases} \min(X) & \text{if step} = 0 \\ \min(x_{\min}, X) & \text{otherwise} \end{cases} \quad (1)$$

$$x_{\min} = \begin{cases} \min(X) & \text{if step} = 0 \\ (1 - c)x_{\min} + c \min(X) & \text{otherwise} \end{cases} \quad (2)$$

The quantization modules keep track of the input tensor’s min and max values,  $x_{\min}$  and  $x_{\max}$ , which are then used to compute  $q_{\min}$ ,  $q_{\max}$ , *zero-point* and *scale* parameters. For both vanilla STE and GC, we study two popular ways of keeping track of these statistics: *min/max*, which tracks the min/max tensor values observed over the course of training; and *momentum*, which computes the moving averages of those statistic during training. The update rules for  $x_{\min}$  for STE *min/max* and STE *momentum* are presented in eq. (1) and eq. (2) respectively, where  $X$  is the tensor to be quantized and  $c$  is the momentum hyperparameter. Equivalent rules apply when updating  $x_{\max}$  (omitted).

## A.4 Degradation Studies

Figures 8 and 9 show the results of the ablation study conducted in section 5 for GCN and GIN. We observe that GCN is more tolerant to INT4 quantization than other architectures. GIN, however, requires accurate representations after the update stage, and heavily suffers from further quantization

like GAT. The idea of performing different stages of inference at different precisions has been proposed, although it is uncommon [42].

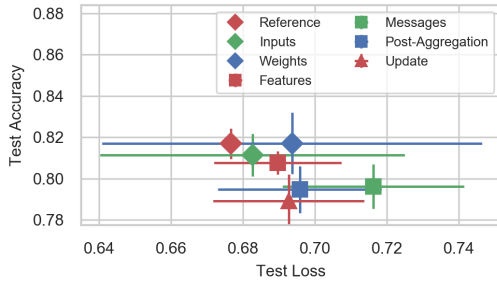


**Figure 8:** Degradation of INT8 GCN on Cora as individual elements are converted to INT4.

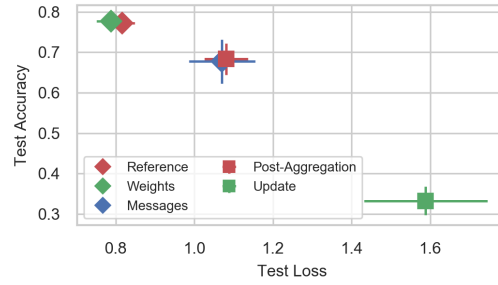


**Figure 9:** Degradation of INT8 GIN on Cora as individual elements are converted to INT4.

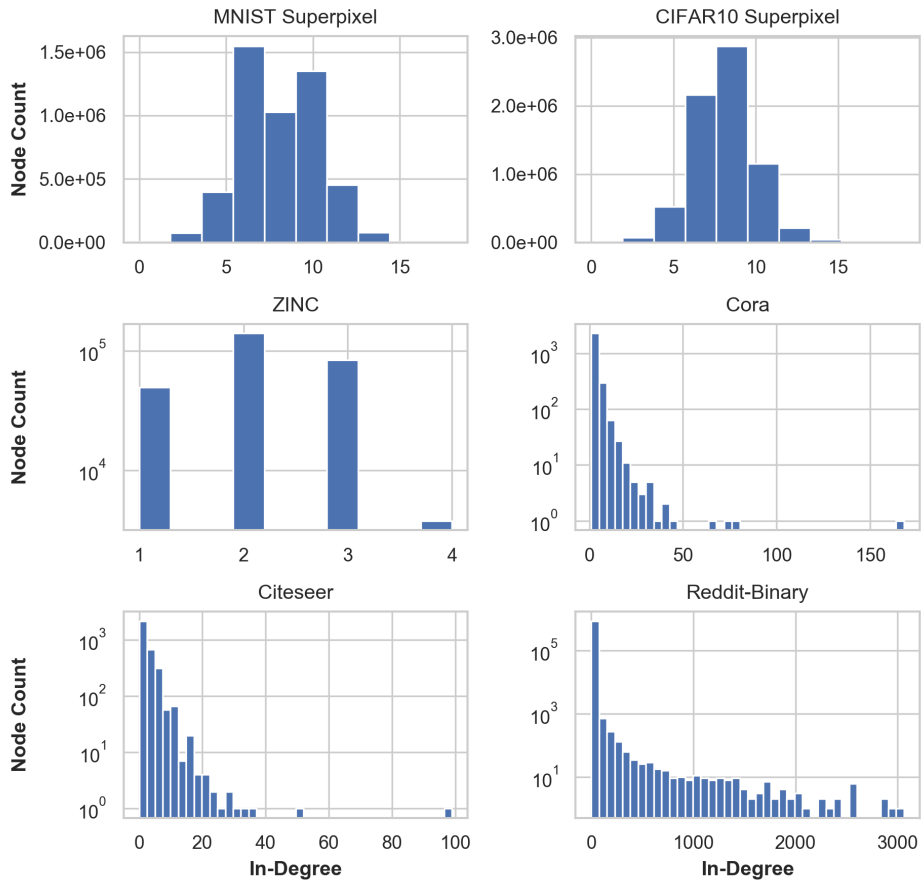


**Figure 10:** In-degree distribution for each of the six datasets assessed. Note that a log  $y$ -axis is used for all datasets except for MNIST and CIFAR-10.

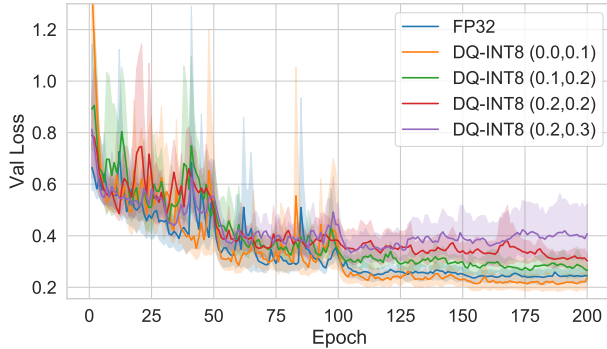


**Figure 11:** Validation loss curves for GIN models evaluated on REDDIT-BINARY. Results averaged across 10-fold cross-validation. We show four DQ-INT8 experiments each with a different values for  $(p_{\min}, p_{\max})$  and our FP32 baseline.

Quantization	Model	REDDIT-BIN $\uparrow$
Ref. (FP32)	GIN	$92.2 \pm 2.3$
Ours (FP32)	GIN	$92.0 \pm 1.5$
DQ-INT8 (0.0, 0.1)	GIN	$91.8 \pm 2.3$
DQ-INT8 (0.1, 0.2)	GIN	$90.1 \pm 2.5$
DQ-INT8 (0.2, 0.2)	GIN	$89.0 \pm 3.0$
DQ-INT8 (0.2, 0.3)	GIN	$88.1 \pm 3.0$

**Table 8:** Final test accuracies for FP32 and DQ-INT8 models whose validation loss curves are shown in fig. 11

Quantization Scheme	Model Arch.	Node Classification		Graph Classification	Graph Regression
		Cora $\uparrow$	Citeseer $\uparrow$	REDDIT-BIN $\uparrow$	ZINC $\downarrow$
QAT-INT8 + DQ	GCN	$80.7 \pm 0.8$	$71.0 \pm 0.7$	-	$0.468 \pm 0.014$
	GAT	$82.1 \pm 0.1$	$70.4 \pm 0.9$	-	$0.462 \pm 0.005$
	GIN	$78.9 \pm 1.2$	$63.8 \pm 3.3$	$77.5 \pm 7.1$	$0.347 \pm 0.028$

**Table 9:** Results obtained with only the stochastic element of Degree-Quant enabled. Percentile-based quantization ranges are disabled in these experiments.